Memorias del Congreso Nacional de Control Automático
ISSN: 2594-2492

Dynamic Characterization of a Reduced Model for the SVC using Dynamic Phasors Approach

Ángel Rodríguez-Chávez, * **Dunstano del Puerto-Flores,** *
Pavel Zuñiga Haro *

* *Department of Mechanical-Electrical Engineering, CUCEI - University of Guadalajara, Jal 44430 Mex (e-mail: jangel.rodriguez@alumnos.udg.mx, dunstano.delpuerto@academicos.udg.mx, pavel.zuniga@cucei.udg.mx).*

Abstract: In this article, a reduced model based on dynamic phasors for the SVC is proposed. By assuming that the connection bus voltage of the SVC is correctly regulated, the capacitor voltage dynamic is neglected. Consequently, a reduction of the differential equation number of the SVC model is achieved. In addition, a comparison is made between a detailed model and the proposed model. The results show that the proposed model has an acceptable performance when the compensator operating modes nearly satisfy the demanded assumption.

Keywords: Dynamic Phasors, SVC, FACTS, Fourier Analysis, Linear System.

1. INTRODUCTION

In the last decades, with the emergence of micro-grids and technological development of devices based on power electronics, more renewable energy technologies such as wind energy and photovoltaic systems have proliferated, (Hossain and Mahmud (2014)). But their stochastic dynamics can bring an improper operation such as voltage fluctuation and power quality, causing instability in the systems, where an effective compensation is necessary for an optimal operation, (Foster et al. (2006)). However, despite the modernity of these systems, the classical *Static VAR Compensator* (SVC) is still a practical option to improve performance. For instance, in (Awad et al. (2017)) the SVC is combined with super-capacitors to mitigate switching overvoltages in micro-grids and in (Kahle et al. (2003)) the SVC compensates very strict requirements of the CERN's Super Proton Synchrotron accelerator.

The SVC is a FACTS device (*Flexible AC Transmission Systems*) that is connected in shunt to the electric power system, and is an alternative equipment to improve transient stability and damping performance for power systems. Its operation is based on power electronics devices that allow flexibility in the control of network parameters, (Hingorani and Gyugyi (2000)). While it is true that the SVC has several advantages, (Hingorani and Gyugyi (2000)), the main challenge is the representation of discrete events in the circuit due to the switching of the power devices and its effect in the dynamics of the capacitor and the inductor. Therefore, the development of simple and accurate models of the SVC is still necessary to efficiently approximate and capture its dynamics, allowing to realize Electromagnetic Transient (EMT) studies and to understand its operation for control design, (Gomes et al. (2006); Zhijun et al. (2009)).

The generalizated state-space averaging method presented in (Sanders et al. (1991)), is the base of the Dynamic Phasors (DP) approach, which is used in this work. DP is a powerful tool for harmonic analysis, which allows the representation of a periodic time-domain in terms of its harmonic components. Moreover, it is an effective tool to characterize commutation devices, like the SVC, allowing a study of the system based on power electronics in the form of a state-space representation, (Almer and Jonsson (2009)). It is also a powerful tool to develop phasor models that are very useful in the analysis of large power systems (Mattavelli et al. (1997)). Dynamic phasor-based models have been developed to perform harmonic studies of electric power systems in order to predict the behavior of the power electronics devices in near periodicity condition obtaining good results, (Kotian and Shubhanga (2015); Gomes et al. (2006)). For instance, since the *Thyristor-Controlled Series Capacitor* (TCSC) and the SVC are based on the TCR, models of the former have been studied to analyze the SVC's behavior.

For the TCSC, in (Mattavelli et al. (1997)) it is proposed a reduced model of the TCSC, by assuming that the line current is always sinusoidal and constant, and the inductor current is symmetrical, where the faster response of the TCR current, *versus* the capacitor voltage one, was

considered.As a result, simple but powerful dynamic models for the TCSC were derived. Afterwards, the harmonic characteristics of this simplified model were presented in (Yun et al. (2009)). Similarly, based on the dual behavior between TCSC and SVC devices, we propose a reduced model for the SVC device. In particular, by assuming that the connection bus voltage is correctly regulated, (*i.e.* the SVC maintains the voltage close to the desired value), the voltage dynamics is considered constant and therefore neglected. Consequently, a reduction of the differential equation number of the SVC model is achieved. Moreover, since the reduced model can be represented in the state-space form, studying its structure is the next step to derive control strategies for the TCR current.

2. DYNAMIC PHASORS

The generalizated state-space averaging method, firstly presented in (Sanders et al. (1991)), is the base of the dynamic phasors approach developed based on the fact that a time-domain signal $x(\tau)$ can be represented, on the time interval $\tau \in (t-T, t]$, using a Fourier series,

$$x(\tau) = \sum_{n=-\infty}^{\infty} \langle x \rangle_n(t) \cdot e^{jn\omega\tau}, \tag{1}$$

where $\omega = (2\pi)/T$, $\langle x \rangle_n$ is the n-th complex time-varying Fourier coefficient and is called *Dynamic Phasor* (DP), with T being the fundamental period, which defines the observation window length that slides over the signal, defined as $\tau \in (t-T, t]$. Hence, if the fundamental period varies, the observation window length too.

The DP's are time-dependent functions, since the interval under consideration slides as a function of time. The n-th dynamic phasor $\langle x \rangle_n$ is defined as,

$$\langle x \rangle_n(t) = \frac{1}{T} \int_{t-T}^{t} x(\tau) \cdot e^{-jn\omega\tau} d\tau, \tag{2}$$

which represents the average over a fundamental period of the signal, the averaging is applied in each cycle of the signal, therefore, the computational resource is reduced.

The following two properties of complex Fourier coefficients are used for harmonic analysis in state-space approach. The *time derivate* of the n-th complex Fourier coefficient satisfies the following equation:

$$\frac{d}{dt}\langle x \rangle_n(t) = \left\langle \frac{d}{dt} x(t) \right\rangle_n - jn\omega \langle x \rangle_n(t). \tag{3}$$

Moreover, if the frequency is varying considerably on time, the approximation of (3) loses accuracy, (Yang et al. (2016)). But for slowly-varying signals in frequency, it is a good approximation to determine the rate of change of the Fourier coefficients, (Sanders et al. (1991)).

The n-th dynamic phasor resulting from the *product of two signals* $x(t)$ and $y(t)$ is defined as,

$$\langle x \cdot y \rangle_n = \sum_{l=-\infty}^{\infty} \langle x \rangle_{n-l} * \langle y \rangle_l, \tag{4}$$

which is equivalent to the discrete convolution of the dynamic phasors of the signals, (Zhijun et al. (2009)). For a real valued signal $x(t)$, the relation between $\langle x \rangle_n$ and $\langle x \rangle_{-n}$ is given for a complex conjugate of $\langle x \rangle_n$ as,

$$\langle x \rangle_{-n} = \langle x \rangle_n^*. \tag{5}$$

The purpose of approaching a time-domain signal in dynamic phasor form is to represent its dynamics in a "quasi-stationary" state. The accuracy approximation depends on the selection of the harmonic components that provide the band-limitation in the frequency-domain, (Mattavelli et al. (1997)).

3. MODEL OF SVC

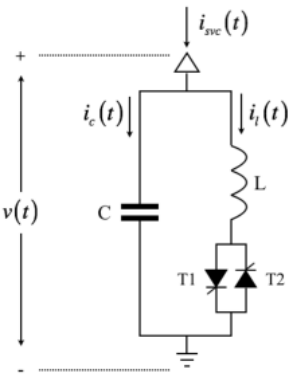

Fig. 1. Circuit diagram of a single-phase SVC.

A basic single-phase SVC is shown in Fig. 1, consisting of a TCR (*Thyristor Controlled Reactor*) in parallel with a fixed capacitor. The TCR comprises an anti-parallel-connected pair of thyristors in series with a linear (air-core) inductor, where the thyristors act as a bidirectional switch due to each thyristor conducts in positive and negative half-cycles of the supply voltage. The following time-domain equations describe the SVC's dynamics,

$$\begin{aligned} C\frac{d}{dt}v_c(t) &= i_{svc}(t) - i_l(t), \\ L\frac{d}{dt}i_l(t) &= q(t)v_c(t), \end{aligned} \tag{6}$$

where v_c represents the capacitor voltage, L is the inductance of the TCR, C is the capacitance, i_l is the inductor current, i_c the capacitor current, i_{svc} is the compensator current, and q is the switching function that denotes the operating state of the thyristors valve: $q = 1$ when one thyristor is in conduction, $q = 0$ when both thyristors are off, (Zhijun et al. (2009); Jusan et al. (2010)).

Assumption 1. The thyristors are considered to be ideal and the operation of both is symmetrical, therefore, only harmonics of odd order will be generated by the TCR.

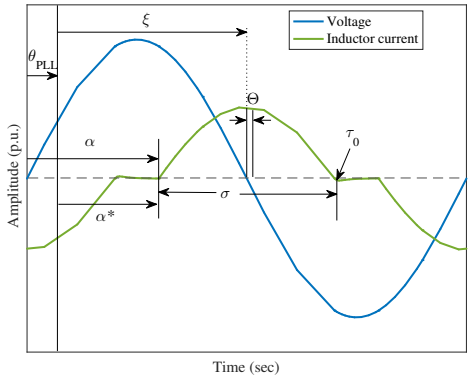

Fig. 2. TCR current and voltage signals form.

Using the dynamic phasors' properties of Section 2, (6) can be rewritten in dynamic phasors terms as follows,

$$C\frac{d}{dt}\langle v_c\rangle_n = \langle i_{svc}\rangle_n - \langle i_l\rangle_n - jn\omega C\langle v_c\rangle_n, \quad (7)$$
$$L\frac{d}{dt}\langle i_l\rangle_n = \langle q\cdot v_c\rangle_n - jn\omega L\langle i_l\rangle_n,$$

where $\langle v_c\rangle_n$ is the n-th voltage dynamic phasor, $\langle i_l\rangle_n$ is the n-th inductor current dynamic phasor and $\langle i_{svc}\rangle_n$ is the n-th compensator current dynamic phasor (time dependence has been suppressed for a compact notation).

Moreover, note that as more Fourier coefficients are considered the number of equations increases; for each differential equation in complex form in (7) are obtained two equations, the real and imaginary part, so it is essential to model only the Fourier coefficients that capture the dynamic behavior for a good approximation of the original signal, (Yun et al. (2009); Zhijun et al. (2009)).

3.1 Modelling of switching function in phasor terms

The function q represents conduction of both thyristors in a period, in a transient-state, the expression is an approximation due to the non-linearity of the components and fundamental operation of devices, *e.g.* PLL (*Phase-Locked Loop*).

Assumption 2. The voltage is essentially sinusoidal and it is taken as the PLL's reference signal for the synchronization of the firing pulses of the thyristors.

Assumption 3. The fundamental component of the inductor current is essentially symmetrical with respect to the zero crossing of the instantaneous voltage, (Jusan et al. (2010); Kotian and Shubhanga (2015)).

The switching function in dynamic phasor terms is modelled based on Fig. 2 and (2) as follows,

$$\langle q\rangle = \begin{cases} \langle q\rangle_0 = \dfrac{\sigma}{\pi} & \text{for n=0} \\ \langle q\rangle_n = \dfrac{\sin(\frac{n\sigma}{2})}{\frac{n\pi}{2}}\cdot e^{-jn(\xi+\Theta)} & \text{for } n\neq 0 \end{cases} \quad (8)$$

where σ is the conduction angle, α is the firing angle of the thyristor, ξ is the phase angle corresponding to the negative zero crossing of the voltage ($\xi = \frac{\pi}{2} - \arg[\langle v\rangle_1]$), σ^* is the conduction angle reference ($\sigma = \sigma^* + 2\Theta$), with $\alpha^* = \xi - \frac{\sigma^*}{2}$, θ_{PLL} is the angle of the PLL and Θ is the gap between the current peak and the zero crossing of the voltage, and in steady-state tends to zero ($\Theta = \arg[\langle i_l\rangle_1\cdot\langle v\rangle_1^*] - \frac{\pi}{2}$). Under Assumption 3, the prevailing conduction angle σ can be approximated as, $\sigma = 2(\pi - \alpha + \theta_{PLL} + \Theta)$. Moreover, the switching function $q(\sigma,\xi,\Theta)$ can be expressed as a function of the components $\langle v\rangle_1$ and $\langle i_l\rangle_1$ and, consequently, (7) renders a state-space model.

In particular, by using the above assumptions and relations, the state-space model (7) in terms of the fundamental frequency DP model is given by,

$$\begin{bmatrix}\langle v_c\rangle_1\\ \langle i_l\rangle_1\end{bmatrix} = \begin{bmatrix} -j\omega & \frac{-1}{C}\\ \frac{\langle q\rangle_0 - \langle q\rangle_2}{L} & -j\omega\end{bmatrix}\begin{bmatrix}\langle v_c\rangle_1\\ \langle i_l\rangle_1\end{bmatrix} + \begin{bmatrix}\frac{1}{C}\\ 0\end{bmatrix}[\langle i_{svc}\rangle] \quad (9)$$

where it has been used,

$$\langle q\cdot v_c\rangle_1 = \langle q\rangle_2\langle v_c\rangle_1^* + \langle q\rangle_0\langle v_c\rangle_1; \quad \langle v_c\rangle_1^* = \langle v_c\rangle_{-1}. \quad (10)$$

3.2 Proposed model

Here, small perturbations around the nominal voltage are assumed to reduce the order of the model in (7). The reduction is based on the fact that, in practice, most modern SVC control systems have an effective voltage control at the nominal or, among the SVC's functions, one is to maintain the voltage between its terminals close to the reference value, (Padiyar (2007)). Analogous model orden reduction of TCSC using the dynamic phasor approach has been proposed in (Mattavelli et al. (1997)), considering that the fundamental phasor of inductor current settles more quickly than the fundamental DP capacitor voltage, which results have motivated this work.

Assumption 4. The disturbances are small around the nominal voltage of the SVC, hence the voltage between compensator terminals remains near constant, the capacitance and inductance are considered to be linear with dependence on the fundamental frequency.

According Assumption 4, the voltage dynamics at the capacitor is neglected, therefore for the dynamics of $\langle v_c\rangle_n$ in (7), it can be approximated as follows,

$$\frac{d}{dt}\langle v_c\rangle_n = \frac{\langle i_{svc}\rangle_n - \langle i_l\rangle_n}{C} - jn\omega\langle v_c\rangle_n = 0, \quad (11)$$

which is replaced in (7), obtaining the expression,

$$\frac{d}{dt}\langle i_l\rangle_n = \left[\frac{\langle q\cdot i_{svc}\rangle_n - \langle q\cdot i_l\rangle_n}{jn\omega LC}\right] - jn\omega\langle i_l\rangle_n. \quad (12)$$

Hence, the SVC can be seen as a variable current source, where the compensator current is a function of the voltage

close to the reference value of the SVC and the equivalent susceptance of the compensator, $i_{svc}(\sigma) = v \cdot B_{svc}(\sigma)$,

$$B_{svc}(\alpha) = B_c + B_{tcr}(\sigma) \begin{cases} B_c = \omega C \\ B_{tcr}(\sigma) = \dfrac{1}{\omega L}\left[\dfrac{\sigma - \sin(\sigma)}{\pi}\right] \end{cases} \quad (13)$$

where B_c is the capacitive susceptance and $B_{tcr}(\sigma)$ represents the equivalent inductive susceptance.

Substituting (13) in (12), the expression of the inductor current is obtained as a function of the variation of the equivalent susceptance of the compensator,

$$\frac{d}{dt}\langle i_l\rangle_n = \left[\frac{\langle q \cdot v\rangle_n \cdot B_{svc}(\alpha) - \langle q \cdot i_l\rangle_n}{jn\omega LC}\right] - jn\omega\langle i_l\rangle_n \quad (14)$$

Remark 1. In the same way that the detailed model, as more Fourier coefficients are considered the number of equations increases, however, this number is reduced in half when assuming a constant bus voltage.

In particular, the state-space form of the proposed model in terms of the fundamental phasors, where $\langle\hat{q}\rangle := \langle q\rangle_0 - \langle q\rangle_2$, is written as follows,

$$\frac{d}{dt}\langle i_l\rangle_1 = \left[\frac{-\langle\hat{q}\rangle}{j\omega LC} - j\omega\right]\langle i_l\rangle_1 + \left[\frac{\langle\hat{q}\rangle \cdot B_{svc}(\alpha)}{j\omega LC}\right]\langle v\rangle_1 \quad (15)$$

4. PERFORMANCE RESULTS OF MODELS

In this section, the simulation results of three SVC models are compared, the detailed circuit based model implemented in MATLAB®/SIMULINK®, hereinafter called Simulink model; the complete dynamic phasors model in (9), hereinafter called the $2n$ model; and the proposed reduced order dynamic phasors model in (15), hereinafter called the n model. The $2n$ model is compared against the Simulink one using the SVC state-variables, that is, the v_c and i_l. For the n model, the comparison against the Simulink model and the $2n$ model is presented for the TCR inductor current only, since the capacitor voltage is assumed to be constant.

All simulations are implemented using the test system shown in Fig. 3, where the capacity of the compensator is ±100MVAr, with L=28.9mH, C=205.85μF, $Z_{tl} = 2 + j1e^{-6}\Omega$ and $V_G = 20$ kV at 60 Hz. An integration time-step of 5 μs with the ode23tb method is used in order to avoid numerical oscillations due to the highly stiff behavior of the commutations, (Hong et al. (2009)).

All simulations consider a firing angle of the thyristors that takes the following values: 90° in 0s-0.4s; 97° in 0.4s-0.8s; 100° in 0.8s-1.2s; 130° in 1.2s-1.6s; and 97° in 1.6s-2s. The signals from the Simulink model are shown as waveforms in the time-domain, whereas the signals from the $2n$ and n models correspond to the harmonic coefficient of the fundamental frequency component of the corresponding signals. The figures that show a harmonic spectrum are obtained through the $2n$ or n model simply by including the corresponding harmonic coefficients.

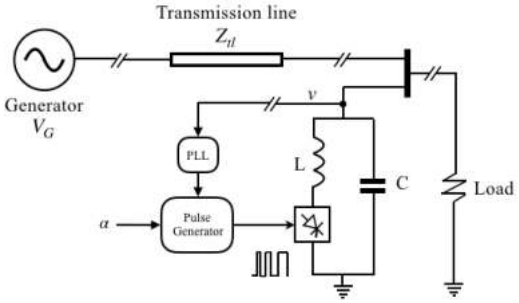

Fig. 3. Study system

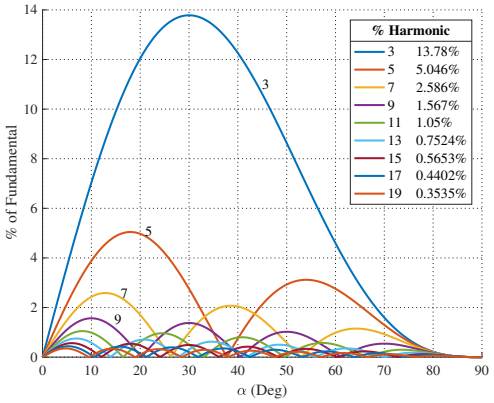

Fig. 4. Harmonics generated in the TCR current

4.1 Simulation results

The TCR acts like an adjustable inductance since the variation of the firing angle changes the fundamental component of the inductor current and consequently its equivalent susceptance, (Hingorani and Gyugyi (2000)). The magnitude of the harmonics in the TCR current due to the distorted waveform caused by the switching of the thyristors (Simulink model) is illustrated in Fig. 4. It is seen that each harmonic component reaches its peak value at a different firing angle, therefore, for each operating condition (firing angle), the harmonics present in the inductor current waveform have a different magnitude.

Due to the action of TCR, the compensator has four operating modes subject to the firing angle: blocking, bypass, capacitive, and inductive mode. When the thyristors are off during each cycle ($\alpha = 180°$) the inductance of the TCR branch is always disconnected from the circuit and the equivalent reactance will be equal to the capacitive reactance of C; it operates in blocking mode. When the thyristors are always on ($\alpha = 90°$) the inductance of the TCR branch is always in the circuit and the equivalent reactance will be equal to the parallel of the inductive and capacitive reactance of L and C, respectively; it operates in bypass mode. When the firing angle (α) has a value between 90° and 180°, the SVC can either be in the

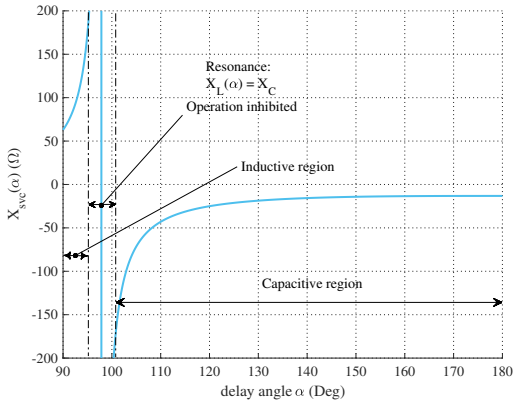

Fig. 5. Impedance characteristic of SVC *vs.* firing angle.

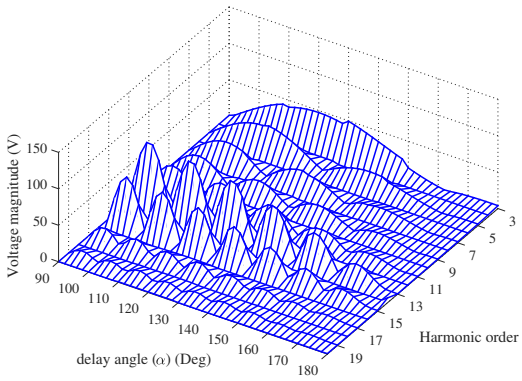

Fig. 7. Harmonic contents in the capacitor voltage

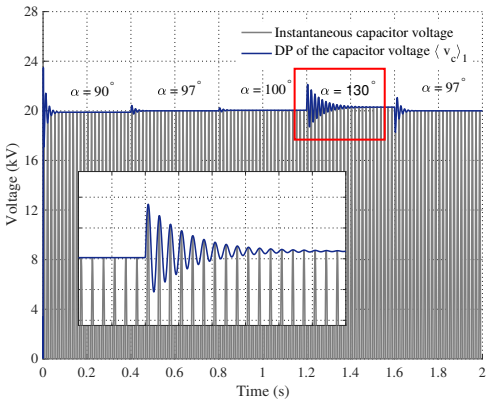

Fig. 6. Capacitor voltage response to step changes in firing angle

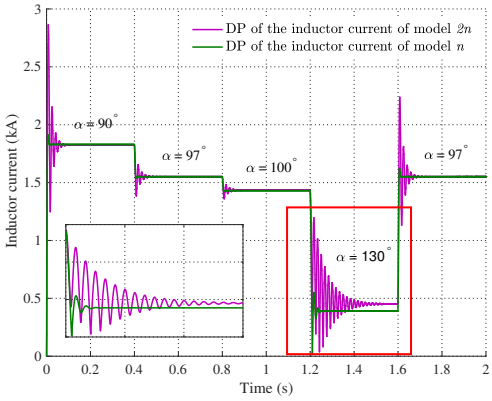

Fig. 8. TCR current dynamic phasor response to step changes in firing angle of model order "$2n$" *versus* current phasor of model order "n".

capacitive or the inductive region, depending on the value of α and the position of the resonance angle.

The operating regions of the SVC are shown in Fig. 5. If the inductive and capacitive reactance are equal, $X_C = X_L(\alpha)$, the equivalent susceptance tends to be infinite, under this condition the SVC operates in resonance mode; this operating point must be avoided since it may lead to instability. In practice, the resonance point can be modified due to the influence of other elements of the network (*e.g.* harmonic filters, transmission lines, FACTS). As the α increases the equivalent inductance decreases, moving away from the resonance to the capacitive region.

Fig. 6 shows the capacitor voltage of the SVC, where it can be seen that the harmonic coefficient accurately tracks the envelope of the instantaneous time-domain voltage. It is important to note that the close tracking of the time-domain signal envelope confirms the accurate performance of the $2n$ model, and that assumptions 2 and 3 are reasonable to consider. The harmonic components of the capacitor voltage are shown in Fig. 7 for different values of α, showing that the dominant harmonics are negligible; non-triplen odd-order.

Fig. 8 shows the fundamental component harmonic coefficient of the TCR current; in this case, for the $2n$ and n models. It can be seen that the results for both models are very similar. The similarity seen from this results show the accuracy of the proposed n model. However, it can be noted that the n model deviates from the $2n$ model when the firing angle of the thyristors is 130°; the capacitor voltage differs the most from the reference value in $\alpha = 130°$, as seen in Fig. 6. That is, the accurate representation of the inductor current fundamental component by the n model is achieved when the capacitor voltage of the SVC is operating close to the bus voltage reference. This result is consistent with Assumption 4 that considers this voltage constant to derive the proposed model; therefore the discrepancy when the capacitor voltage deviates from the reference one. This also impacts the transient response of the dynamic phasor of model n, which loses accuracy compared to the $2n$ model due to elimination of the capacitor voltage dynamics.

The harmonic content of the TCR for different values of α is shown in Fig. 9, where again only odd order harmonics are present; it can be seen that as α increases, the mag-

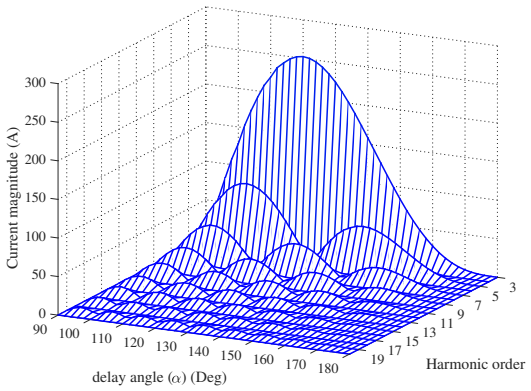

Fig. 9. Harmonic content in the TCR current

nitude of the harmonics decreases since the conduction angle becomes smaller.

5. CONCLUSION

This paper presented a reduced model of the SVC device using the dynamic phasors approach. By assuming that the connection bus voltage is correctly regulated, (*i.e.* the SVC maintains the bus voltage close to the reference value), the capacitor voltage dynamic is neglected. Consequently, a reduction of the differential equation number of the SVC model is achieved. The proposed model has well tracked the envelope, with respect to the detailed model, of the inductor current waveform, when the compensator operates nearly on the capacitive region. But the reduced model leaks accuracy in the presence of large voltage variations. However, in practice there are safety limits that do not allow large voltage variations, therefore model n and model $2n$ could be used to estimate the original time-domain signal of the state variables.

Currently, works toward improvement on the reduced model response are carried out by a slight refinement in the evaluation of $\langle q \cdot v \rangle_1$ or $\langle q \cdot i_l \rangle_1$ in (15). Namely, rather than using only the fundamental component to represent v or i_l for this evaluation, an extended expression with significant harmonic content will be consider, similarly as in (Mattavelli et al. (1997)). At the same time, applications for power factor control, reactive power compensation, and voltage regulation based on the model n are being developed.

ACKNOWLEDGEMENTS

D. del Puerto Flores is supported in part by the Mexican PRODEP project UDG-PTC-1319. D. del Puerto-Flores and Pavel Zuñiga Haro are supported in part by the internal project PROSNI-2018.

REFERENCES

Almer, S. and Jonsson, U. (2009). Dynamic Phasor Analysis of Periodic Systems. *IEEE Trans. on Autom. Control*, 54(8), 2007–2012.

Awad, E.A., Badran, E.A., and Youssef, F.H. (2017). Mitigation of Switching Overvoltages in Microgrids Based on SVC and Supercapacitor. *IET Gener. Trans. Distrib.*, 12(2), 355–362.

Foster, S., Xu, L., and Fox, B. (2006). Grid Integration of Wind Farms Using SVC and STATCOM. In *International Universities Power Eng. Conf.*, 157–161.

Gomes, S., Martins, N., and Stankovic, A. (2006). Improved Controller Design using New Dynamic Phasor Models of SVC's Suitable for High Frequency Analysis. In *IEEE PES Transm. and Distrib. Conf. and Exhibition*, 1436–1444.

Hingorani, N.G. and Gyugyi, L. (2000). *Understanding FACTS*. IEEE press.

Hong, S.N., Liu, C.R., Bo, Z.Q., and Klimek, A. (2009). Elimination of Numerical Oscillation of Dynamic Phasor in HVDC System Simulation. In *IEEE PES General Meeting*, 1–5.

Hossain, J. and Mahmud, A. (2014). *Large Scale Renewable Power Generation*. Springer.

Jusan, F.C., Gomes, S., and Taranto, G.N. (2010). SSR results obtained with a dynamic phasor model of SVC using modal analysis. *International Journal of Electrical Power & Energy Systems*, 32(6), 571 – 582.

Kahle, K., Pedersen, J., Larsson, T., and Magalhaes de Oliveira, M. (2003). The New 150 MVAr, 18 kV Static Var Compensator at CERN: Background, Design and Commissioning. In *Inter. Conf. on Electricity Distribution*.

Kotian, S.M. and Shubhanga, K.N. (2015). Dynamic Phasor Modelling and Simulation. In *IEEE India Conference*, 1–6.

Mattavelli, P., Verghese, G.C., and Stankovic, A.M. (1997). Phasor Dynamics of Thyristor-Controlled Series Capacitor Systems. *IEEE Trans. on Power Syst.*, 12(3), 1259–1267.

Padiyar, K.R. (2007). *FACTS Controller in Power Transmission and Distribution*. New Age Inter. (P) Limited.

Sanders, S.R., Noworolski, J.M., Liu, X.Z., and Verghese, G.C. (1991). Generalized Averaging Method for Power Conversion Circuits. *IEEE Trans. on Power Electronics*, 6(2), 251–259.

Yang, T., Bozhko, S., Le-Peuvedic, J.M., Asher, G., and Hill, C.I. (2016). Dynamic Phasor Modeling of Multi-Generator Variable Frequency Electrical Power Systems. *IEEE Trans. on Power Syst.*, 31(1), 563–571.

Yun, L., Liu, D., Zhou, C., Zhang, L., and Du, X. (2009). Modeling and Simulation of TCSC with Dynamic Phasors Considering Harmonic Characteristics. In *Int. Conf. on Energy and Environment Tech.*, 176–179.

Zhijun, E., Fang, D., Chan, K., and Yuan, S. (2009). Hybrid simulation of power systems with SVC dynamic phasor model. *International Journal of Electrical Power & Energy Systems*, 31(5), 175 –180.

